
Figures and figure supplements

Identification of RBPMS as a mammalian smooth muscle master splicing regulator via proximity of its gene with super-enhancers

Erick E Nakagaki-Silva *et al*

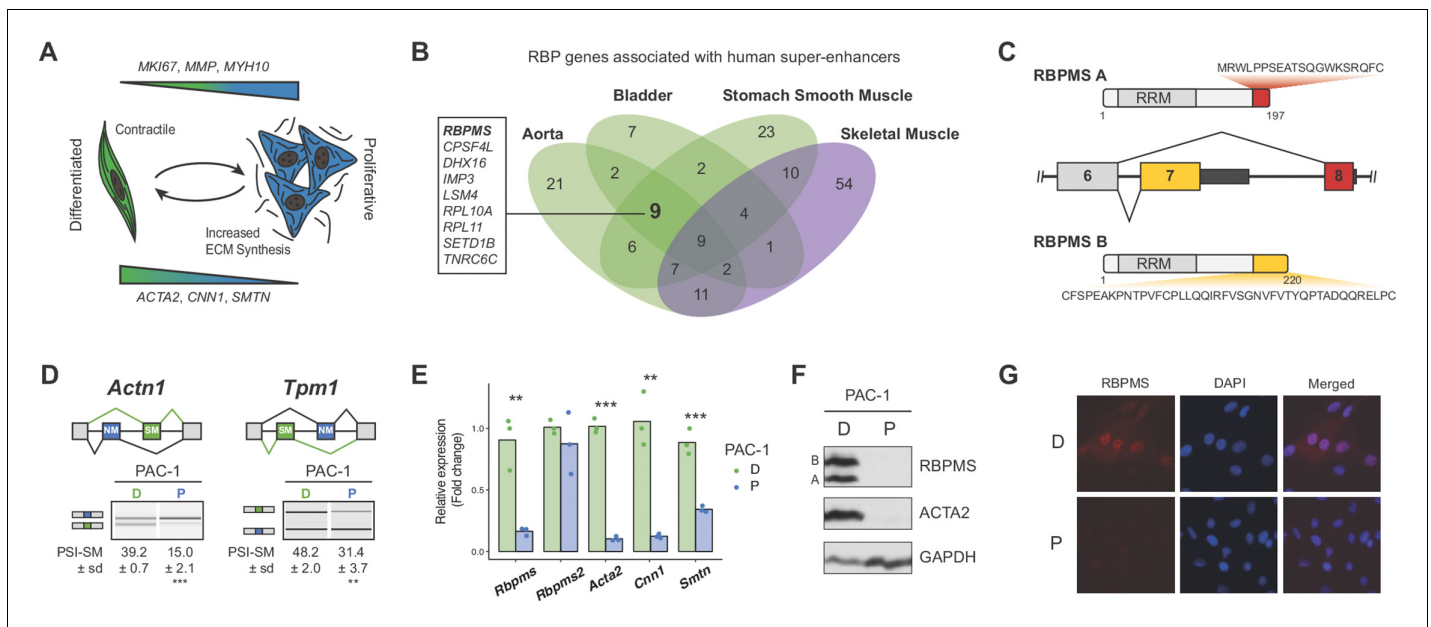


Figure 1. RBPMS is associated with SMC super-enhancers and is highly expressed in the differentiated PAC1 cells. (A) Diagram of the SMC dedifferentiation. SMC markers of differentiation and dedifferentiation are respectively shown at the bottom and top of the diagram. (B) Venn diagram of RBP genes associated with super-enhancers across different human smooth muscle tissues. Skeletal muscle was used as an outlier. RBPs common to all smooth muscle tissues but not skeletal muscle are shown on the left. (C) Schematic of the AS event determining the two major RBPMS isoforms, RBPMS A (red) and RBPMS B (yellow). (D) RT-PCR analysis of SMC splicing markers, *Actn1* and *Tpm1*, in differentiated (D) and proliferative (P) PAC1 cells. Schematic of the regulated mutually exclusive splicing events on top and respective isoforms products on the left. Values shown are the quantified PSI (percent spliced in) of the smooth muscle isoforms (SM) \pm standard deviation ($n = 3$). (E) qRT-PCR analysis of *Rbpms* (all isoforms), *Rbpms2* and SMC differentiation markers *Acta2*, *Cnn1* and *Smtn*, in PAC1 cells D (green) and P (blue). Expression was normalized to the average of two housekeepers (*Gapdh* and *Rpl32*) and the mean of the relative expression is shown ($n = 3$). Each point shows data from an individual sample. Statistical significance was performed using Student's t-test (* $p < 0.05$, ** $p < 0.01$, *** $p < 0.001$). (F) Western blots for RBPMS in D and P PAC1 cells. ACTA2 is a SMC differentiation marker and GAPDH a loading control. A and B indicates the two RBPMS isoforms. (G) Immunofluorescence in D and P PAC1 cells for RBPMS. DAPI staining for nuclei.

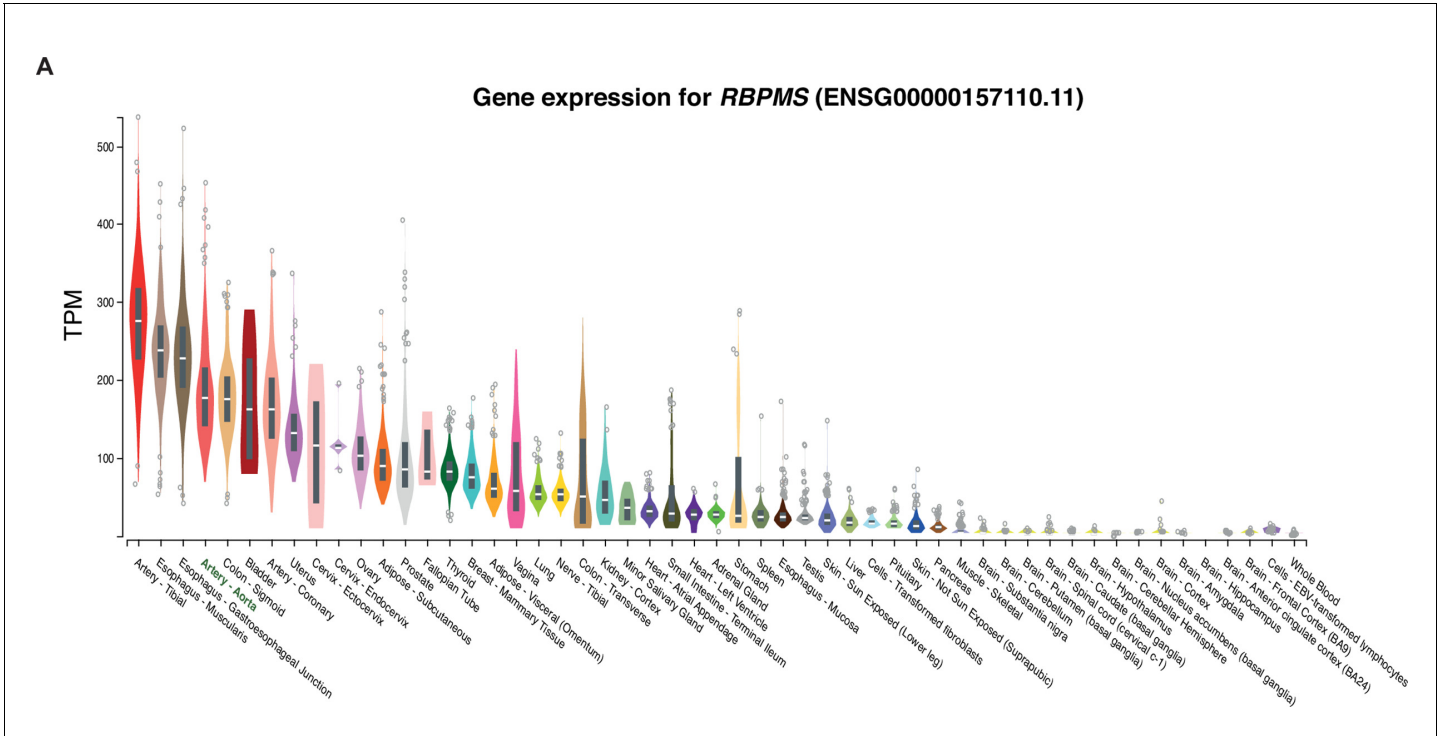


Figure 1—figure supplement 1. *RBPM5* is highly expressed in SM tissues. (A) *RBPM5* mRNA expression across different human tissues in the GTEx database (GTEx Consortium, 2013). TPM: transcripts per million.

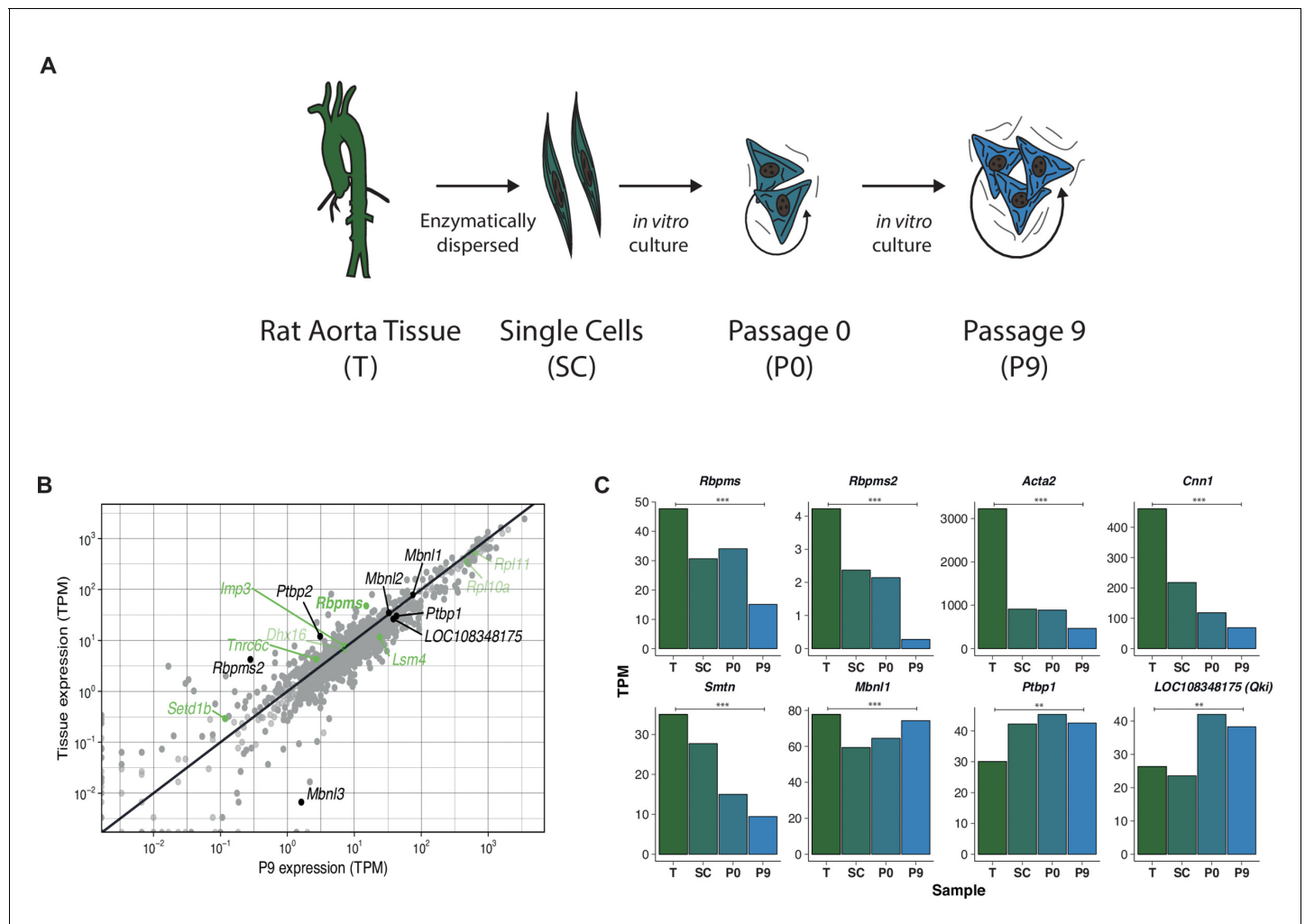


Figure 1—figure supplement 2. mRNA abundance analysis of the rat aorta SMC de-differentiation RNA-Seq. **(A)** Schematic of the experimental design of the rat aorta tissue dedifferentiation. **(B)** mRNA abundance of RBP genes in differentiated aorta tissue (T) and proliferative passage 9 (P9). RBPs whose genes were found associated with smooth muscle tissue super-enhancers (**Figure 1B**) are highlighted in green. Additionally, other well characterized RBPs and *Rbpms2* are labelled in black. *LOC108348175* is the Ensembl annotated rat *Qki* like gene. Statistical significance in mRNA abundance changes between T and P9 was calculated by DESeq2 and is indicated in dark and light gray color ($\text{padj} < 0.05$ and non-significant changes respectively). mRNA levels are expressed in transcripts per million (TPM). *Cpsf4l* gene was not found in this dataset. **(C)** mRNA abundance changes measured in transcripts per million (TPM) during rat aorta dedifferentiation (T, SC, P0 and P9). Genes shown are *Rbpms* and its paralog *Rbpms2*, SMC differentiation markers, *Acta2*, *Cnn1* and *Smtn*, and other RBPs, *Mbnl1*, *Ptbp1* and *Qki*.

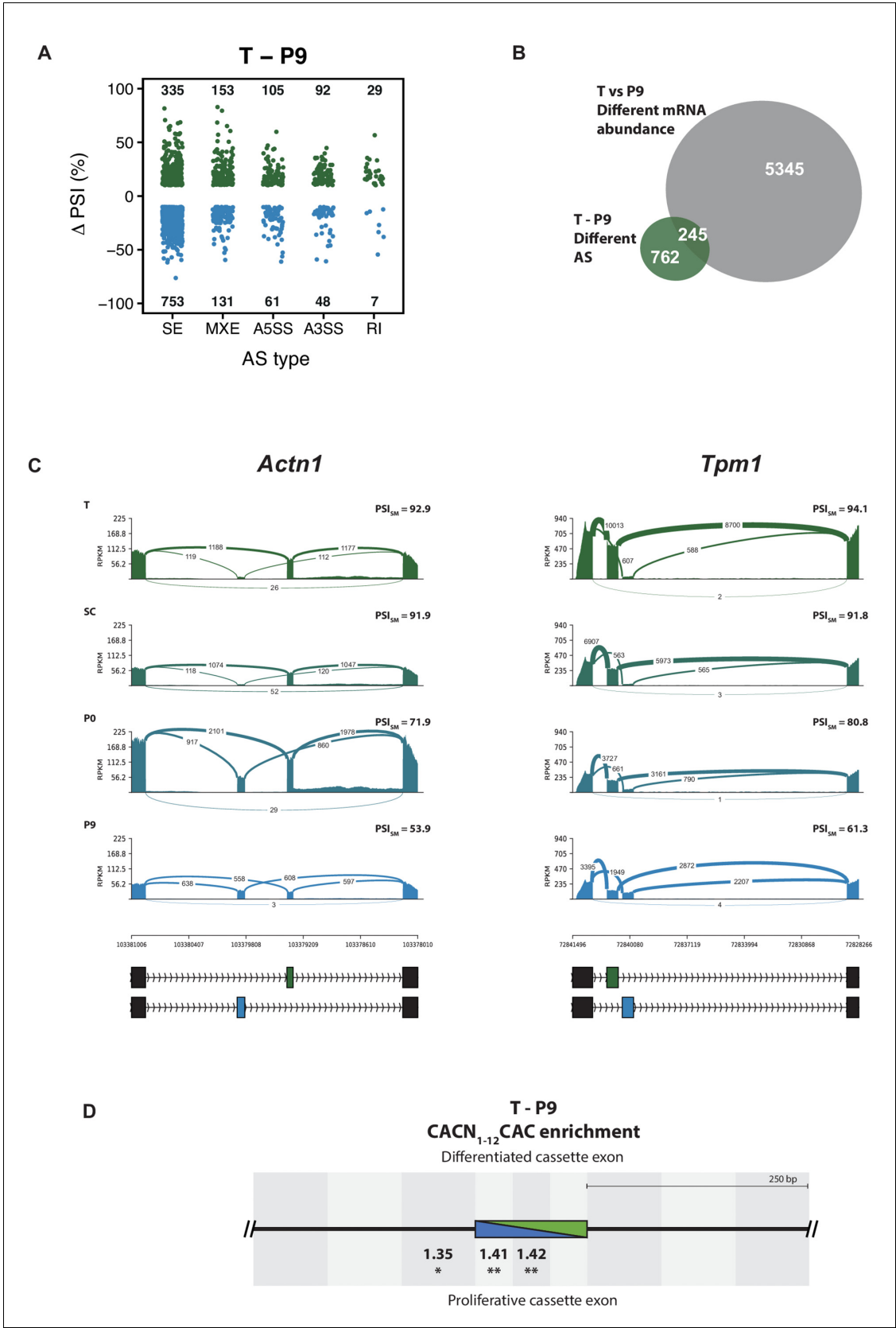


Figure 1—figure supplement 3. Alternative splicing analysis of the rat aorta SMC de-differentiation RNA-Seq. (A) AS changes when comparing T and P9 conditions. Only significant ASE with FDR < 0.05 and ΔPSI greater than 10% are shown. ASE were classified as skipped exons (SE), mutually exclusive

Figure 1—figure supplement 3 continued on next page

Figure 1—figure supplement 3 continued

exons (MXE), 5' and 3' alternative splice sites (A5SS and A3SS) and retained intron (RI). The number of events differentially alternatively spliced are shown in the graph. **(B)** Overlap of the number of genes affected at the levels of mRNA abundance and AS in the T and P9 comparison. **(C)** Sashimi plot of the SMC mutually exclusive splicing markers, *Actn1* and *Tpm1*, in rat aorta tissue dedifferentiation. PSI values represent the mean of the PSI values calculated by rMATS. **(D)** RBPMS motif enrichment in differentially alternatively spliced SE in the T and P9 comparison. A pair of CAC separated by 1 to 12 nt was used as the RBPMS motif. Values indicate the motif enrichment. Statistical significance was calculated by the Matt tool (* $p < 0.05$, ** $p < 0.01$, *** $p < 0.001$).

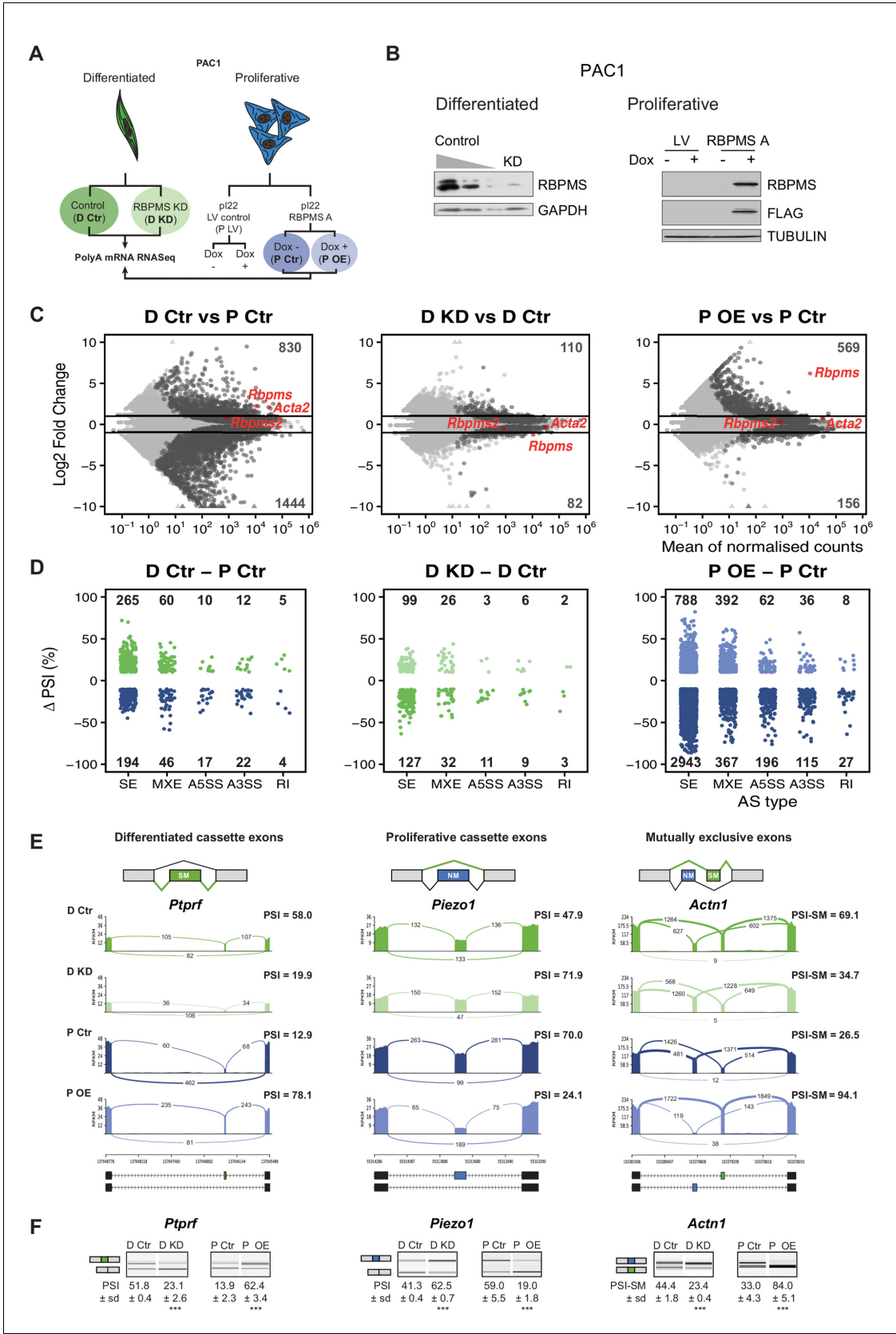


Figure 2. RBPMS regulates AS in PAC1 cells. (A) Schematic of experimental design of RBPMS knockdown and overexpression in PAC1 cells. (B) Western blots for RBPMS in PAC1 knockdown, left, and inducible lentiviral overexpression, right. FLAG antibodies were also used for the

Figure 2 continued on next page

Figure 2 continued

overexpression of 3xFLAG tagged RBPMS. GAPDH and TUBULIN were used as loading controls. (C) MA plots of alterations in mRNA abundance in PAC1 dedifferentiation, left, RBPMS knockdown, middle, and RBPMS A overexpression, right. Dark gray: genes with significant changes ($p\text{-adj} < 0.05$). Light gray: genes with $p\text{-adj} \geq 0.05$. Red: *Rbpms*, *Rbpms2* and the SMC marker, *Acta2*. Numbers of up and down-regulated are shown at top and bottom. Horizontal lines; \log_2 fold change = 1 and -1 . (D) AS changes ($\text{FDR} < 0.05$ and ΔPSI greater than 10%) in PAC1 cell dedifferentiation, left, RBPMS knockdown, middle, and RBPMS A overexpression, right. ASE were classified into skipped exon (SE), mutually exclusive exon (MXE), alternative 5' and 3' splice site (A5SS and A3SS) and retained intron (RI) by rMATS. Numbers indicate the number of significant ASE of each event type between the conditions compared. (E) Sashimi plots of selected ASEs. *Ptprf* is shown as a differentiated cassette exon (green), *Piezo1* as a proliferative cassette exons (blue) and *Actn1* as a MXE. The numbers on the arches indicate the number of reads mapping to the exon-exon junctions. PSI values for the ASE are indicated for each condition. Values correspond to the mean PSI calculated by rMATS. In the case of the *Actn1* MXE, the percent inclusion of the SM exon is shown (PSI-SM). Schematic of the mRNA isoforms generated by the alternative splicing are found at the bottom as well as the chromosome coordinates. (F) RT-PCR validation of ASEs from panel E. Values shown are the mean of the PSI \pm standard deviation ($n = 3$). Statistical significance was calculated using Student's t-test (* $p < 0.05$, ** $p < 0.01$, *** $p < 0.001$). See **Figure 2—figure supplement 3** for more ASEs validated in the RBPMS knockdown and RBPMS A overexpression by RT-PCR.

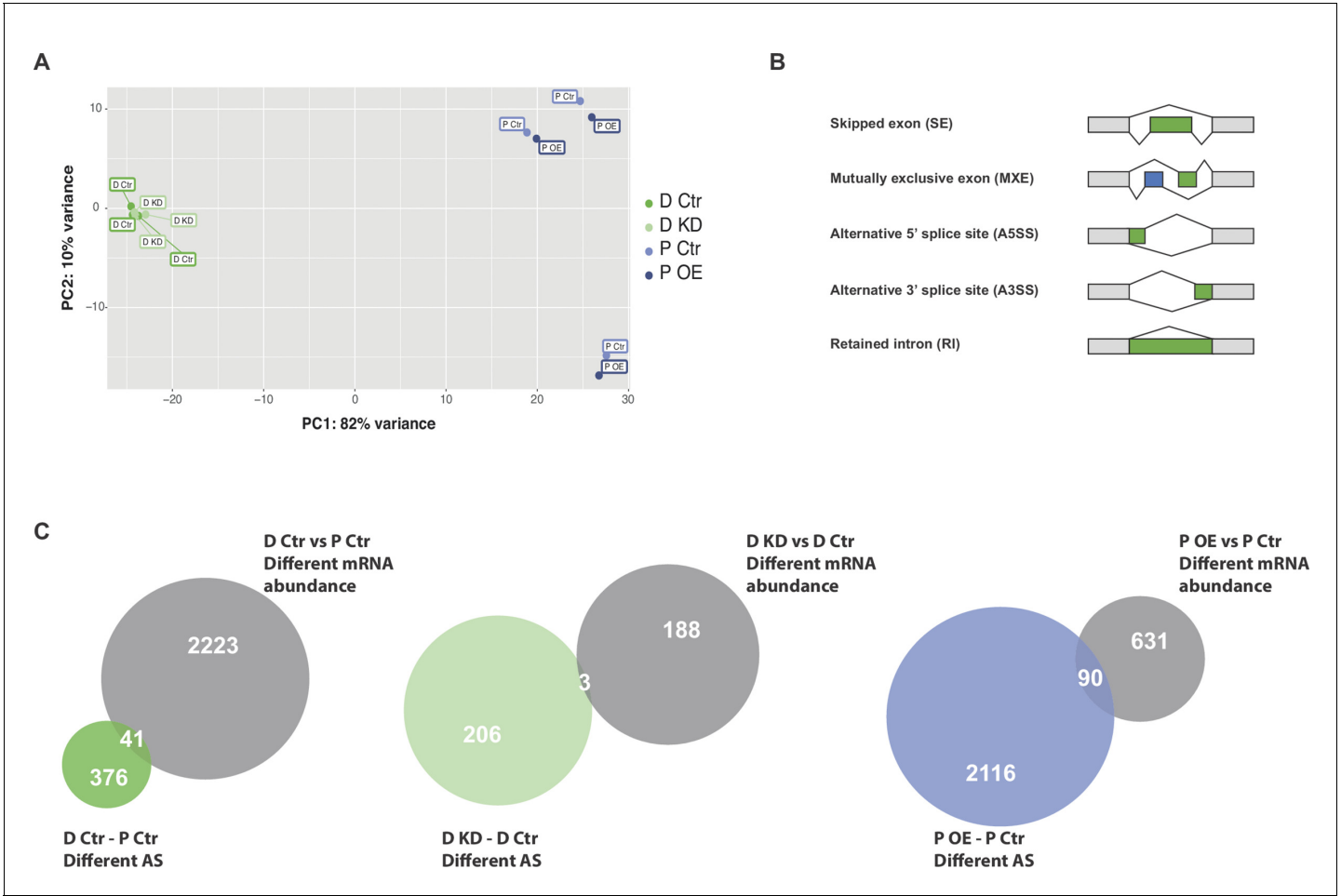


Figure 2—figure supplement 1. Principal Component Analysis of PAC1 RNAseq samples and overlap of genes regulated at the splicing and abundance levels. **(A)** Principal Component Analysis (PCA) based upon mRNA abundance variance of RBPMS knockdown (D Ctr and D KD) and overexpression (P Ctr and P OE) replicates. **(B)** Schematics of the different AS types detected by rMATS. **(C)** Overlap of the number of genes affected at the levels of mRNA abundance and AS in the PAC1 dedifferentiation and RBPMS knockdown and overexpression comparisons.

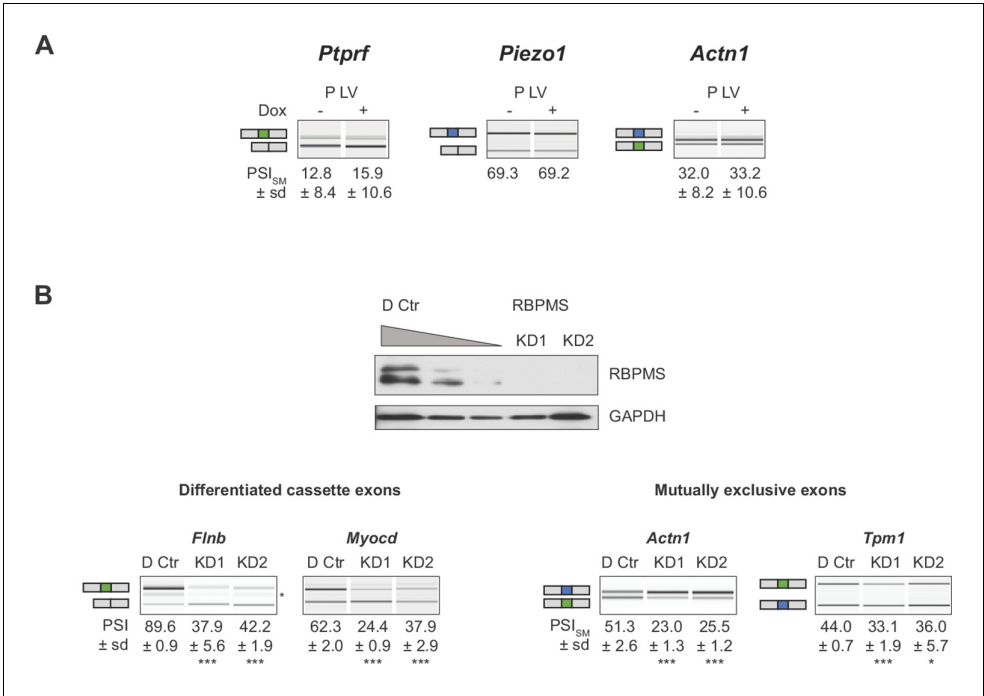


Figure 2—figure supplement 2. AS changes of SM genes are specific to RBPMS expression. (A) Validation of lack of regulated splicing in lentiviral control populations (P LV) upon doxycycline treatment. (B) Validation of a second RBPMS siRNA (KD2, Stealth siRNAs, Thermo Fisher Scientific (RSS363829): CGCUUCGAUCCUGAAAUCCCGCAA). Western blot probing for RBPMS in differentiated PAC1 cells treated with one of the siRNAs. GAPDH was used as a loading control in the western blot. RNAs were extracted and RT-PCR carried out to validate the ASE previously characterized for KD1. In (A) and (B), values shown are the mean ± sd of PSI (n = 3). Statistical significance was calculated using Student’s t-test (*p<0.05, **p<0.01, ***p<0.001).

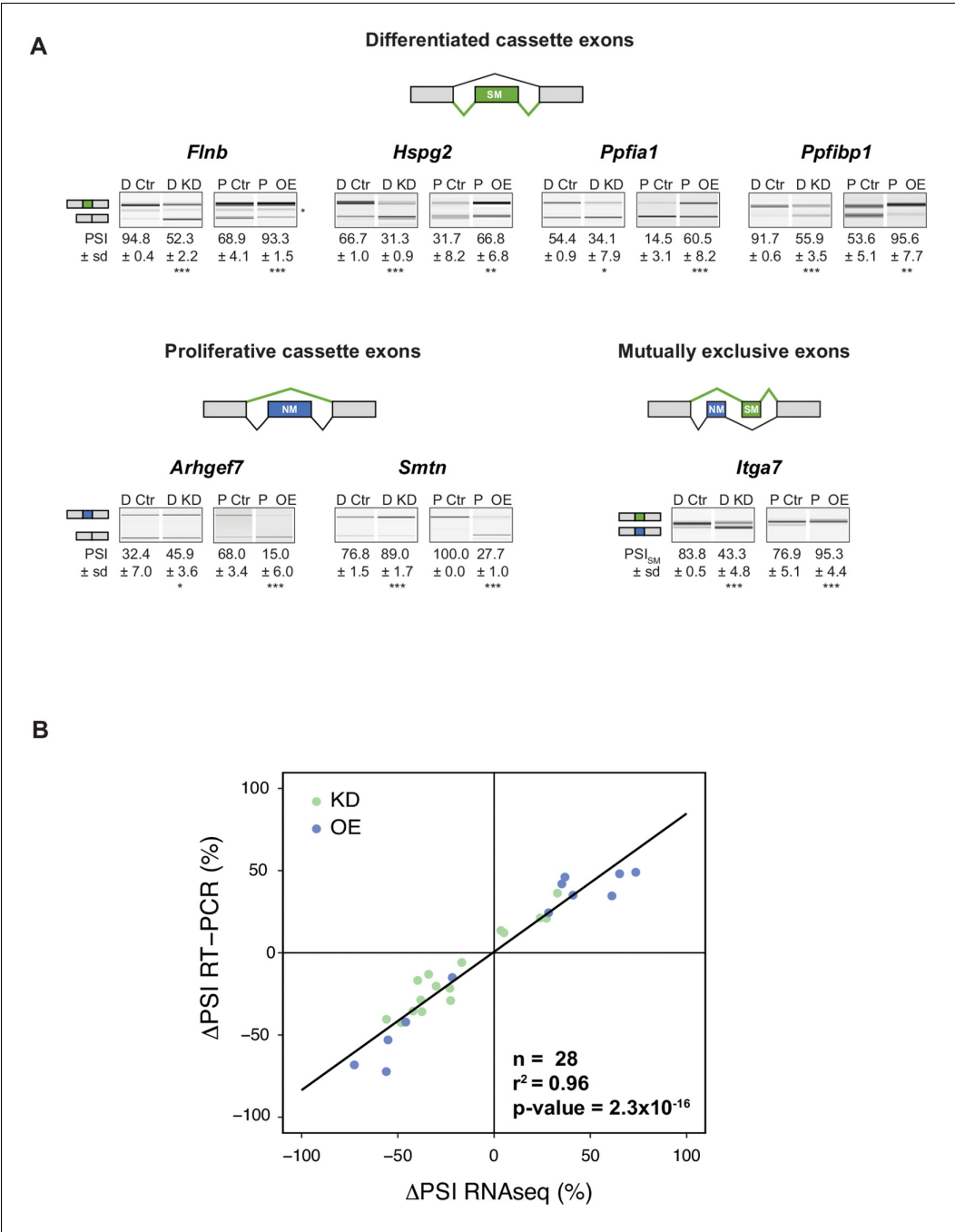


Figure 2—figure supplement 3. Δ PSI values determined by RT-PCR and RNA-Seq show good agreement. (A) Validation of differentiated and proliferative cassette and mutually exclusive splicing events by RT-PCR for both RBPMS knockdown and overexpression. Schematics indicate the splicing isoform corresponding to the PCR product. Values shown are the mean \pm sd of PSI (n = 3). Statistical significance was calculated using Student's t-test (* $p < 0.05$, ** $p < 0.01$, *** $p < 0.001$). (B) PSI correlation between the estimated Δ PSI from the rMATS analysis of the RBPMS knockdown and overexpression RNAseq experiments and the observed Δ PSI from the RT-PCR validations of RBPMS experiments (n = 28). Black line indicates the linear regression model. For statistical significance, a Pearson correlation test was carried out in RStudio and the results are shown in the right corner of the plot. r^2 is the correlation coefficient and the p-value indicates the statistical significance of the correlation.

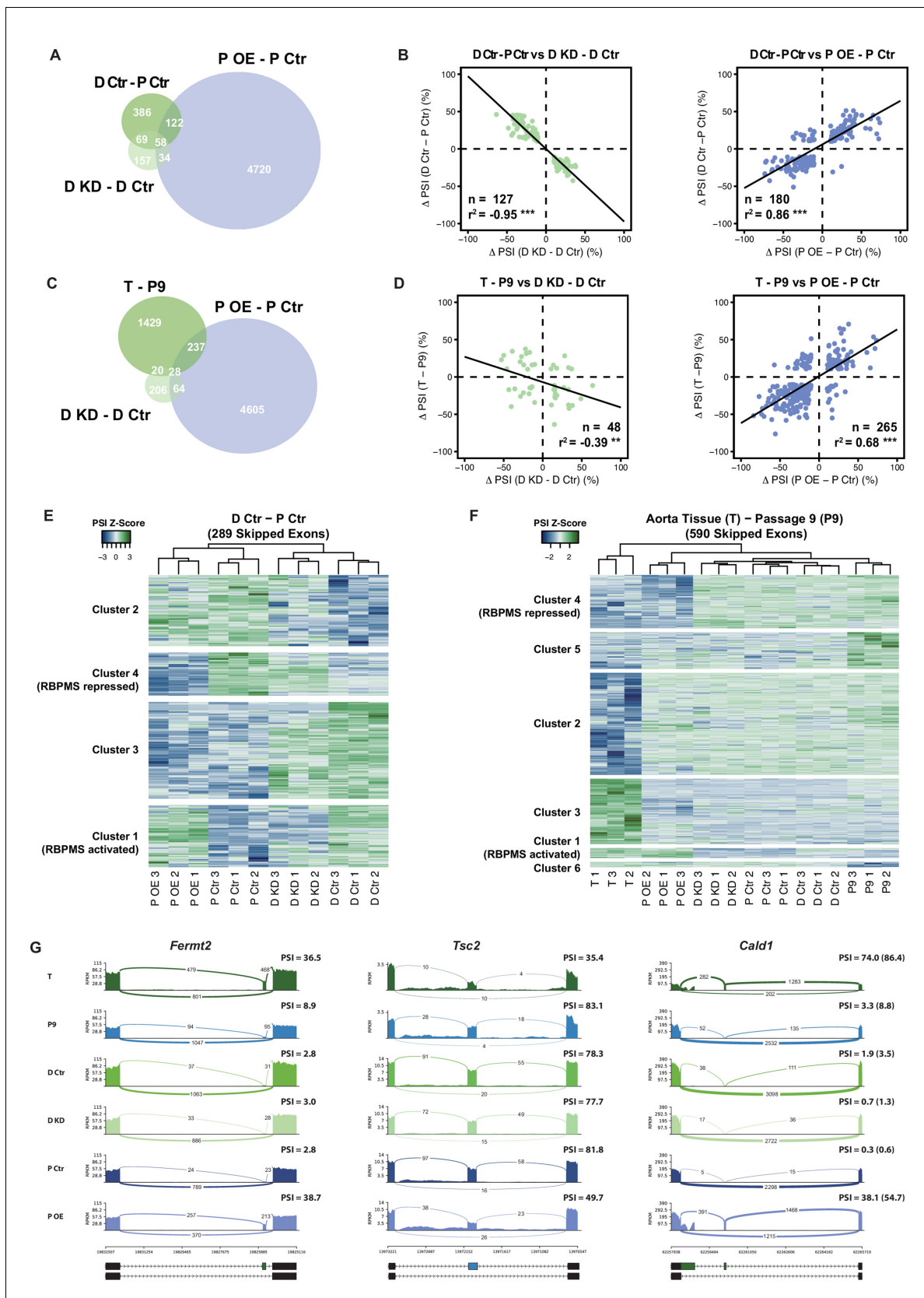


Figure 3. RBPMs recapitulates the AS program of differentiated PAC1 and aorta tissue. (A) Venn diagram of significant AEs (FDR < 0.05 and Δ PSI cutoff of 10%) identified in the PAC1 dedifferentiation, RBPMs knockdown and RBPMs A overexpression comparisons. (B) Δ PSI correlation of Figure 3 continued on next page

Figure 3 continued

overlapping ASEs (FDR < 0.05 and Δ PSI cutoff of 10%) from the PAC1 cells dedifferentiation and RBPMS knockdown, left, or RBPMS A overexpression, right. The line indicates the linear regression model. Statistical significance was carried out by Pearson correlation test. n is the number of ASEs assessed, r^2 is the correlation coefficient. Statistical significance of the correlation: * p <0.05, ** p <0.01, *** p <0.001. (C) Venn diagram of significant ASEs identified in RBPMS knockdown, overexpression and aorta tissue to passage nine comparisons. (D) Δ PSI correlation of overlapping ASEs from the rat aorta tissue dedifferentiation and RBPMS knockdown, left, or RBPMS A overexpression, right. (E) Heatmap of 289 SEs regulated in the PAC1 dedifferentiation comparison (D Ctr - P Ctr). Each column represents a replicate sample (1-3) from RBPMS knockdown (D Ctr and D KD) or overexpression (P Ctr and P OE). Rows are significant SE events from PAC1 dedifferentiation. Rows and columns were grouped by hierarchical clustering. Blue and green colors in the Z-score scaled rows represent low and high PSI values respectively. (F) Heatmap of 590 SEs regulated in the rat aorta tissue dedifferentiation comparison (T - P9). Each column represents one sample from either aorta tissue dedifferentiation (T and P9), RBPMS knockdown (D Ctr and D KD) or RBPMS overexpression (P Ctr and P OE). Rows are significant SE events from the T - P9 comparison. Rows and columns were grouped by hierarchical clustering. Blue and green colors in the Z-score scaled rows represent low and high PSI values respectively. (G) Sashimi plots of selected ASEs highly regulated in the aorta tissue and RBPMS overexpression. *Fermt2* is an RBPMS activated exon from Cluster one in panel F. *Tsc2* is an RBPMS repressed exon from Cluster 4 of panel E. *Cald1* has an RBPMS activated exon 4 and downstream five splice site on exon 3b. For *Cald1*, a manually calculated PSI in parentheses takes into account the A5SS which was not included in the rMATS annotation.

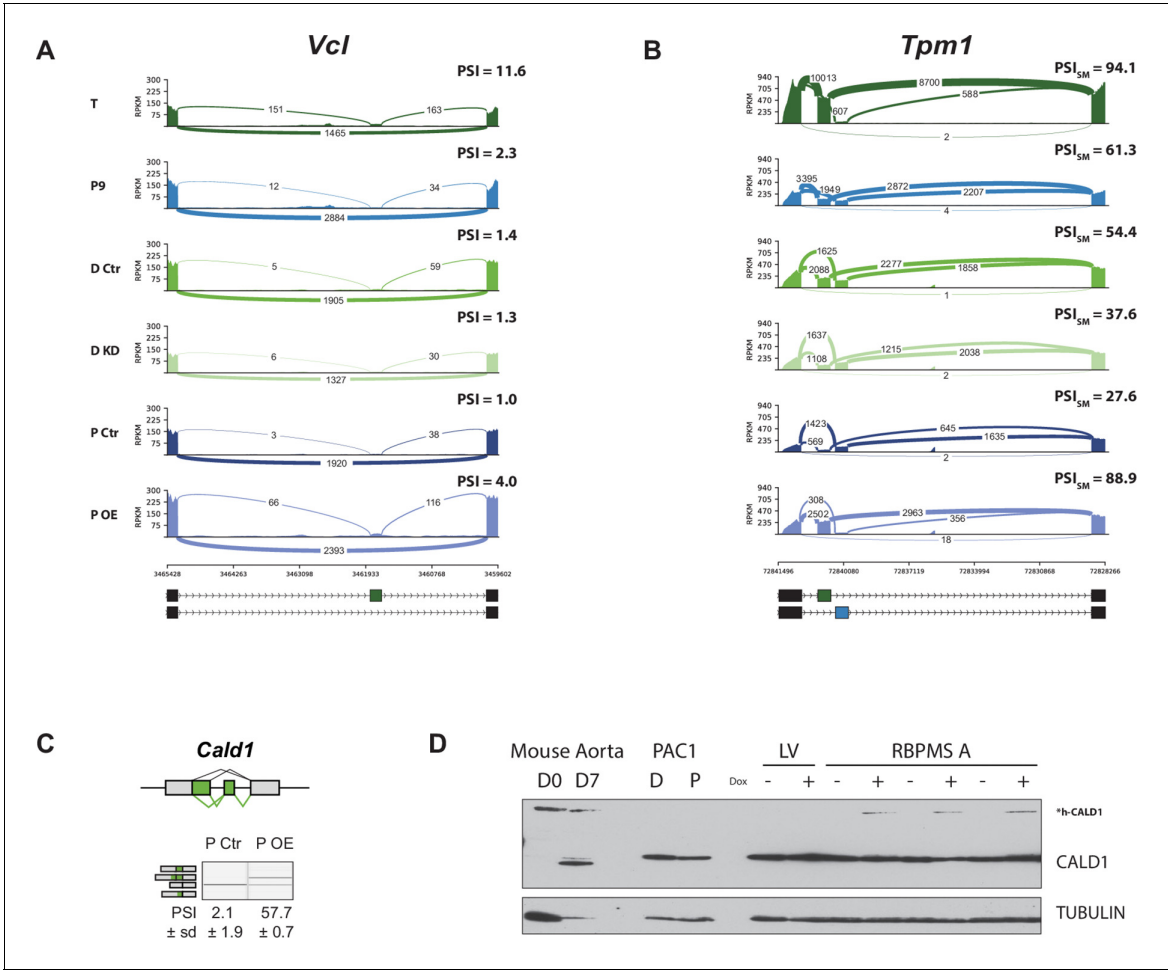


Figure 3—figure supplement 1. RBPMS recapitulates the aorta tissue AS pattern of *Vcl*, *Tpm1* and *Cald1*. **(A)** Sashimi plot of the *Vcl* cassette exon regulated during aorta tissue dedifferentiation ($FDR < 4 \times 10^{-14}$) and by RBPMS overexpression ($FDR < 1.2 \times 10^{-12}$). PSI values represent the mean of the PSI values calculated by rMATS analysis. **(B)** Sashimi plot of the *Tpm1* mutually exclusive exon regulated during aorta tissue dedifferentiation and by RBPMS overexpression. PSI values represent the mean of the PSI values calculated by rMATS analysis for the SM exon 2. **(C)** RT-PCR validation of *Cald1* ASE (A5SS and SE) in the RBPMS overexpression in proliferative PAC1 cells. Schematic of the *Cald1* ASE and *Cald1* isoforms amplified in the PCR are shown on the top and left, respectively. **(D)** Western blot probing for CALD1 showing the appearance of the h-CALD1 protein isoform upon RBPMS overexpression. The specificity of the isoform switch was also confirmed in *Mus musculus* differentiated (D0) and proliferative (D7) SMC samples from aorta tissue. The larger smooth muscle specific isoform of CALD1 is indicated by h-CALD1. Values shown are mean \pm sd ($n = 3$) of the PSI. Statistical significance was calculated using Student's t-test (* $p < 0.05$, ** $p < 0.01$, *** $p < 0.001$).

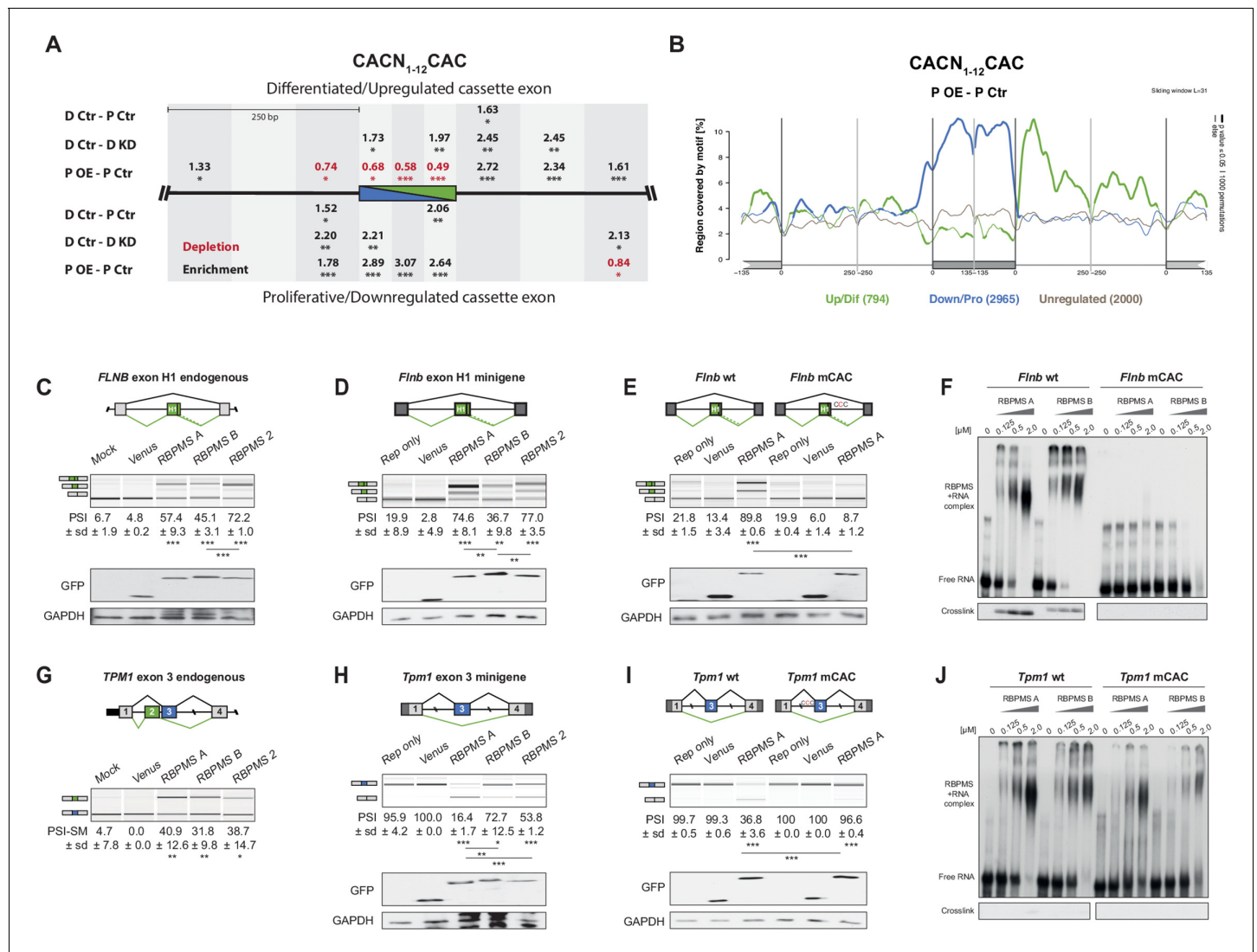


Figure 4. RBPMS directly regulates exons associated with CAC motifs. **(A)** RBPMS motif (CACN₁₋₁₂CAC) enrichment in differentially alternatively spliced cassette exons in the PAC1 dedifferentiation (D Ctr - P Ctr), RBPMS knockdown (D Ctr - D KD) and RBPMS overexpression (P OE - P Ctr) comparisons. Values indicate degree of motif enrichment (black) or depletion (red). Statistical significance: *p<0.05, **p<0.01, ***p<0.001. **(B)** RBPMS motif (CACN₁₋₁₂CAC) map from RBPMS overexpression (P OE - P Ctr). Upregulated (green), downregulated (blue) and unregulated (gray) cassette exons are shown. Statistical significance: p<0.05, 1000 permutations is indicated by thicker line width. **(C)** RBPMS overexpression in HEK293 cells and RT-PCR of endogenous *FLNB* exon H1 splicing. Schematic of *Flnb* exon H1 as a differentiated cassette exon activated by RBPMS. The splicing pattern of *FLNB* was tested upon overexpression of Venus tagged RBPMS A, B and 2. A mock and a Venus control were also tested in parallel. **(D)** Effect of RBPMS overexpression on rat *Flnb* splicing reporter in HEK293 cells. Schematic of the *Flnb* reporter and RT-PCR for the splicing patterns of *Flnb* reporter upon coexpression of RBPMS isoforms and RBPMS2. **(E)** *Flnb* reporter with point mutations disrupting RBPMS motifs (CAC to CCC) were tested for RBPMS A regulation. Left, wild-type reporter and right, mutant CAC reporter (mCAC) RT-PCRs. **(F)** Electric mobility shift assay (EMSA) for in vitro binding of recombinant RBPMS A and B to in vitro transcribed wild-type and mCAC RNAs of *Flnb* exon H1 downstream intron sequence (top left and right). Lower panel: UV-crosslinking of same samples. **(G)** RBPMS overexpression in HEK293 cells and RT-PCR of endogenous *TPM1* MXE exon 2 and 3 splicing. The splicing pattern of *TPM1* was tested upon overexpression of Venus tagged RBPMS A, B and 2. A mock and a Venus control were also tested in parallel. **(H)** Effect of RBPMS overexpression on rat *Tpm1* splicing reporter in HEK293 cells. Schematic of the *Tpm1* reporter and RT-PCR for the splicing patterns of *Tpm1* reporter upon RBPMS isoforms and RBPMS2. **(I)** *Tpm1* reporter with point mutations disrupting RBPMS motifs (CAC to CCC) was tested for RBPMS A regulation. Left, wild-type reporter and right, mutant CAC reporter (mCAC) RT-PCRs. **(J)** In vitro binding of recombinant RBPMS A and B to in vitro transcribed wild-type and mCAC RNAs of *Tpm1* exon three upstream intron sequence. EMSA, top and UV crosslinking, bottom. In **(F)** and **(J)**, in vitro binding assays were carried out using recombinant protein in a serial dilution (1:4) in a range of 0.125 to 2 μ M. In panels **(C-E)** and **(G-I)**, values are the mean PSI \pm sd (n = 3). For *Flnb* cassette exon, the PSI is the sum of both short and long isoforms generated by a A5SS event. For *Tpm1* MXE, the SM exon PSI is shown (PSI-SM). Schematics of the splicing isoforms indicate the PCR products, differentiated (green) and proliferative (blue). Statistical significance was calculated using Student's t-test (*p<0.05, **p<0.01, ***p<0.001). Western blot anti-GFP and GAPDH, loading control, were carried out

Figure 4 continued on next page

Figure 4 continued

to assess RBPMS isoform overexpression in HEK293 (panels C-E, H, I). The western blot in (C) is also a representative of (G), since both RT-PCRs (*FLNB* and *TPM1*) are from the same overexpression experiment.

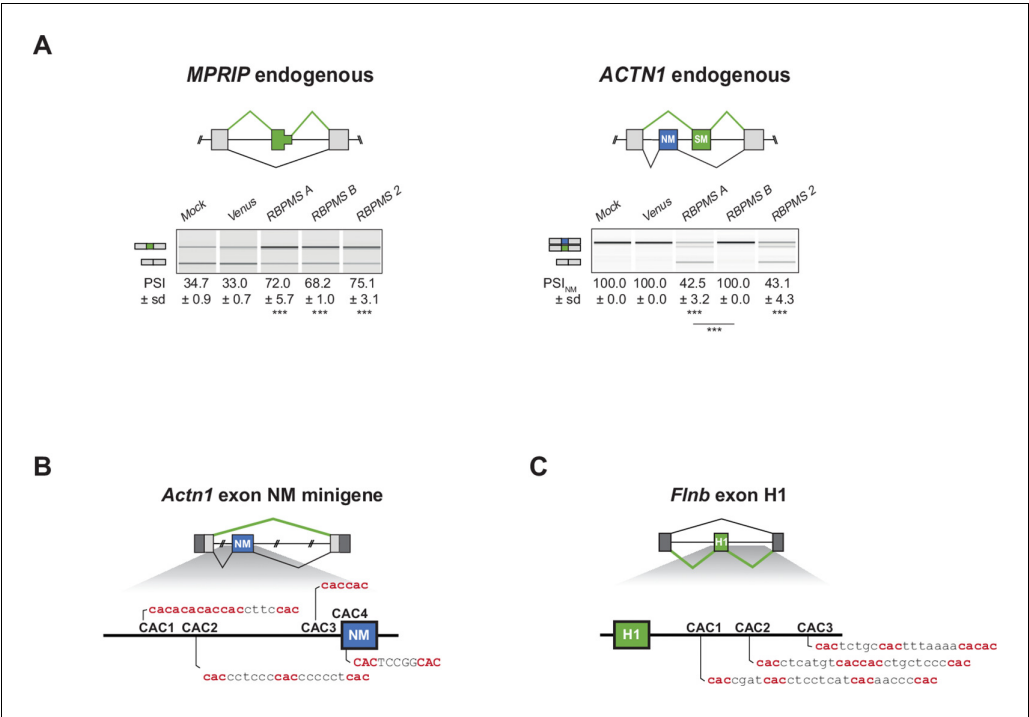


Figure 4—figure supplement 1. RBPMS promotes the SM splicing of *MPRIP* and *ACTN1* in HEK293 cells. (A) RT-PCR validation of endogenous *MPRIP* and *ACTN1* ASEs upon RBPMS isoform and RBPMS2 overexpression in HEK293 cells. Schematics of *MPRIP* SE and *ACTN1* MXE are found at the top. (B) Schematic of potential RBPMS CAC motifs upstream of *Actn1* exon NM and (C) downstream of *Flnb* exon H1.

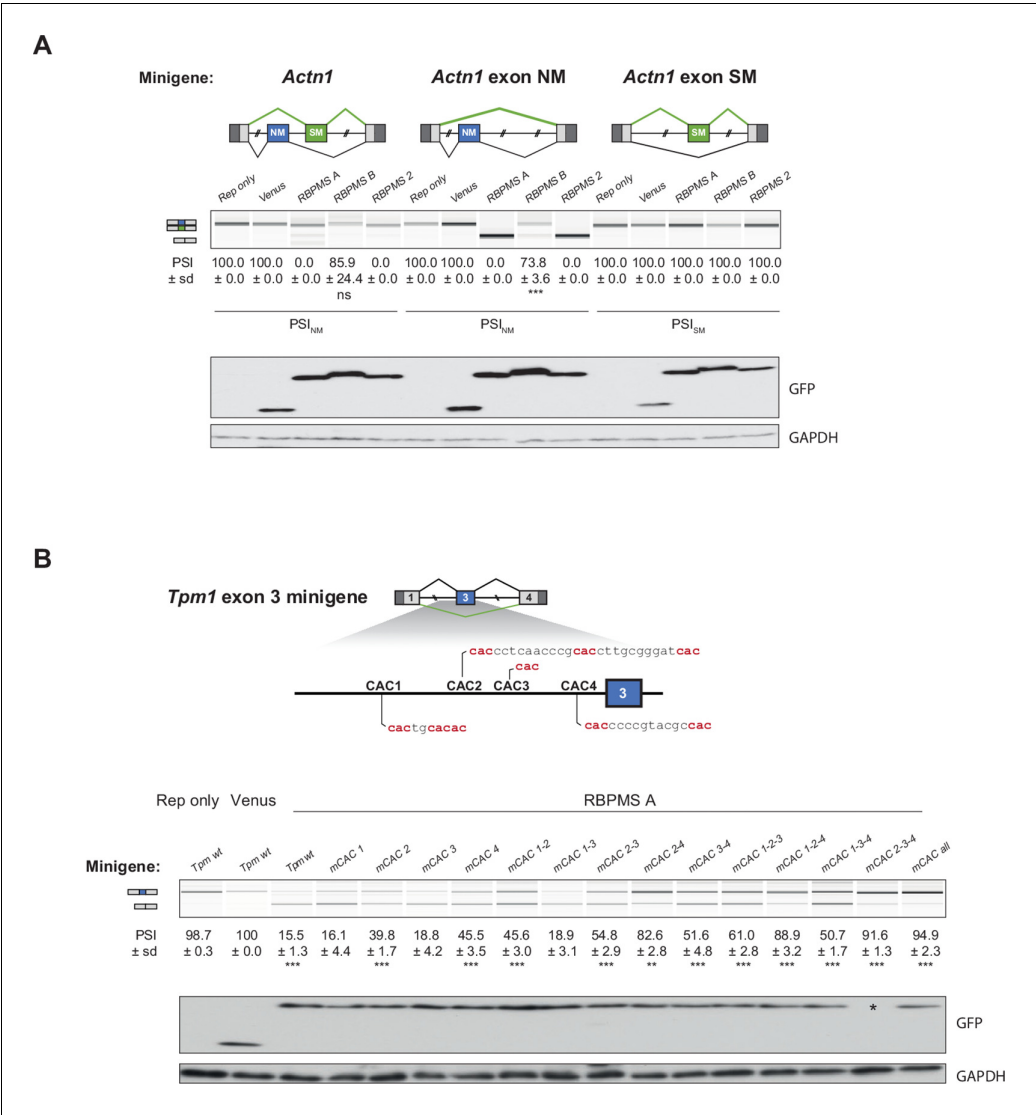


Figure 4—figure supplement 2. RBPMS represses the splicing of the NM exon of *Actn1* and *Tpm1*. (A) *Actn1* splicing upon RBPMS overexpression in HEK293 cells. *Actn1* reporters containing both the SM and NM exons or only the SM or NM exon were tested upon RBPMS overexpression. Schematics of the different *Actn1* splicing reporters tested are shown at the top. Western blot to verify RBPMS overexpression were probed for GFP and GAPDH as a loading control. (B) Mapping RBPMS cis elements in the *Tpm1* exon three splicing reporter. Potential RBPMS CAC motifs upstream of exon three are highlighted in the schematic at the top. Combinations of different CAC mutations were tested for RBPMS A overexpression in HEK293 cells. Overexpression was assessed by western blot probing for GFP (Venus) and GAPDH as a loading control. No overexpression was detected in the lane marked “*” although the PSI differs from the reporter only lane. In (A) and (B), schematics of the splicing isoforms identify the PCR products and values shown are mean ± sd (n = 3) of PSI. In case of MXE the SM exon inclusion is shown. Statistical significance was calculated using Student’s t-test (*p<0.05, **p<0.01, ***p<0.001).

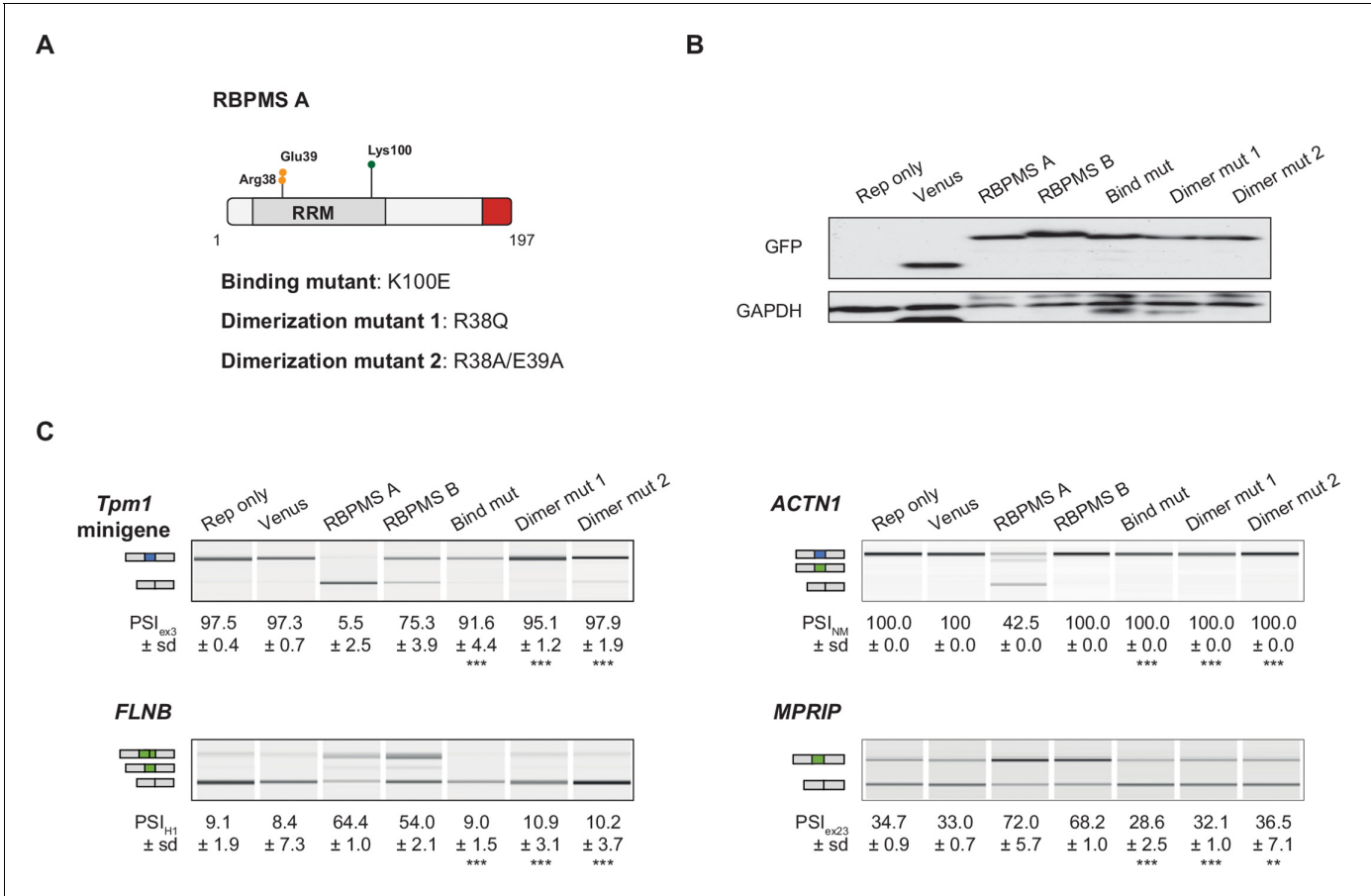


Figure 4—figure supplement 3. RBPMs splicing activity requires RNA binding and dimerization. (A) Schematic of RBPMs isoform A with residues mutated in the binding and dimerization mutants highlighted. (B) Western blot probing for GFP to assess overexpression of RBPMs isoforms and mutants in HEK293 cells. GAPDH was used as a loading control. (C) RT-PCR of RBPMs splicing targets (*Tpm1* minigene and endogenous *FLNB*, *ACTN1* and *MPRIIP*) upon overexpression of wild type RBPMs isoforms and RBPMs A mutants in HEK293 cells. Schematics indicate the splicing isoform corresponding to the PCR product. Values shown are the mean ± sd of PSI (n = 3). Statistical significance was calculated using Student’s t-test (*p<0.05, **p<0.01, ***p<0.001).

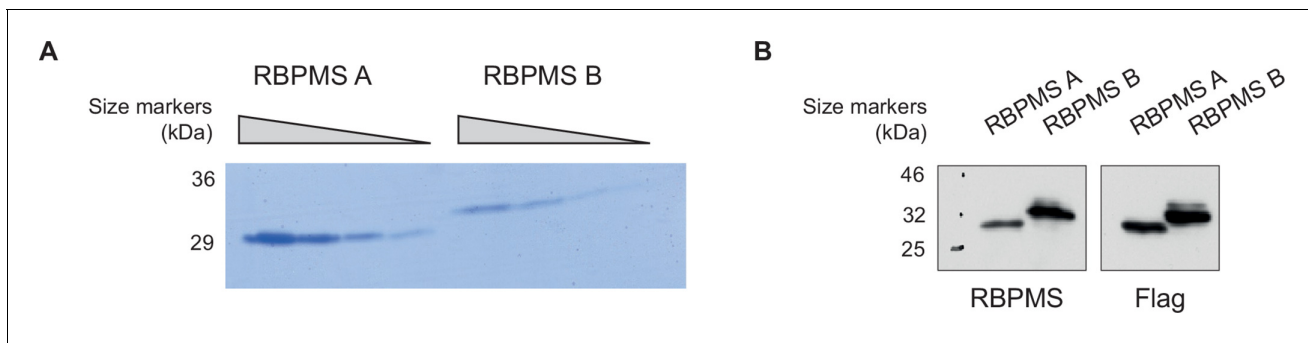


Figure 4—figure supplement 4. RBPMS recombinant proteins. (A) RBPMS A and B recombinant proteins. Purified recombinant RBPMS A and B were analyzed in a 20% denaturing polyacrylamide gel. A BSA titration was run in parallel for quantification of the recombinant protein. (B) Recombinant protein sequences were confirmed by western blot probing for RBPMS and FLAG.

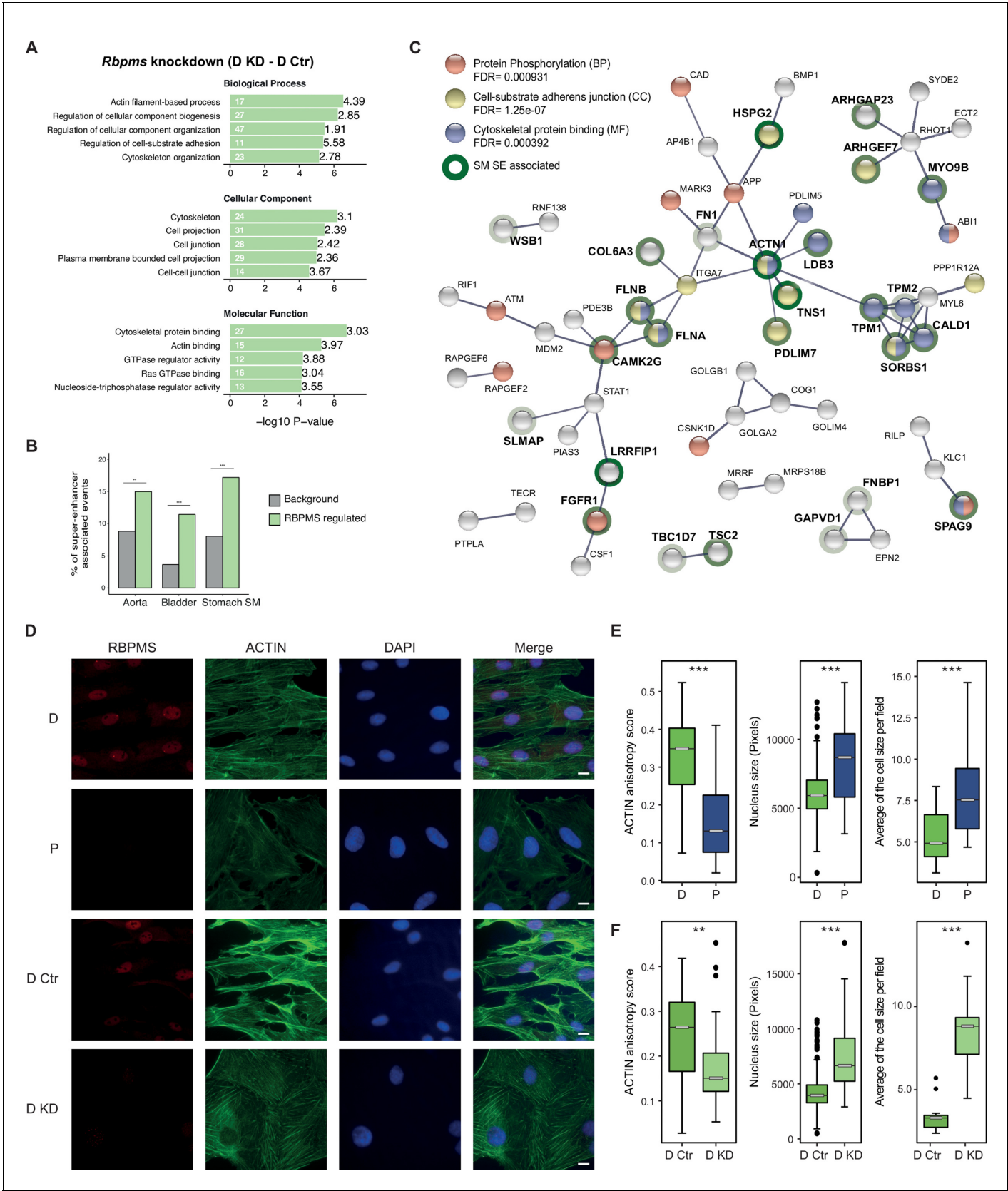


Figure 5. RBPMS regulates functionally important targets in SMCs. (A) GO analysis of genes with cassette exons regulated in RBPMS knockdown. The top five enriched GO terms in the three categories (biological process, molecular function and cellular component) are shown. Values within and in Figure 5 continued on next page

Figure 5 continued

front of the bars indicate the number of genes in the enriched term and the enrichment relative to the background list. **(B)** Enrichment of exons regulated by RBPMS knockdown within genes associated with super-enhancers in smooth muscle tissues. Background set is all cassette exon events (regulated and unregulated) detected by rMATS in the same experiment. Significance determined by hypergeometric P-value. **(C)** PPI network of genes showing concordant splicing regulation upon RBPMS knockdown and PAC1 differentiation status, combined with genes concordantly regulated by RBPMS overexpression and in aorta tissue datasets. PPI network was generated in STRING using experiments and database as the sources of interactions. Network edges represent the interaction confidence. Enriched GO terms (BP, biological process, MF, molecular function and CC, cellular component) were also included in the analysis and are indicated in red, blue and yellow. Super-enhancer associated gene names are in bold and are highlighted gray, light green or dark green shading according to whether they were super-enhancer associated in 1, 2 or 3 SMC tissues. **(D)** Immunofluorescence of RBPMS and actin (Phalloidin) in differentiated and proliferative PAC1 cells (D and P) and upon prolonged (120 hr) RBPMS knockdown in differentiated PAC1 cells (D Ctr and D KD). DAPI staining for cell nuclei. Scale bars 10 μ m. **(E)** Left, anisotropy measurement of actin fibers in PAC1 cells D (differentiated) and P (proliferative) using the FibrilTool ImageJ macro (n = 44 and 52). Middle, nucleus size measurement shown in pixels (n = 182 and 130). Right, average of the cell size quantified per field (n = 11 and 15). **(F)** Left, anisotropy measurement of actin fibers in RBPMS knockdown (D Ctr and D KD) using the FibrilTool ImageJ macro (n = 56 and 33). Middle, nucleus size measurement shown in pixels (n = 363 and 75). Right, average of the cell size quantified per field (n = 14 and 10). In **(E)** and **(F)**, statistical significance was obtained from a Mann-Whitney-Wilcoxon Test (*p<0.05, **p<0.01, ***p<0.001). Data shown are from one representative experiment carried out in triplicate.

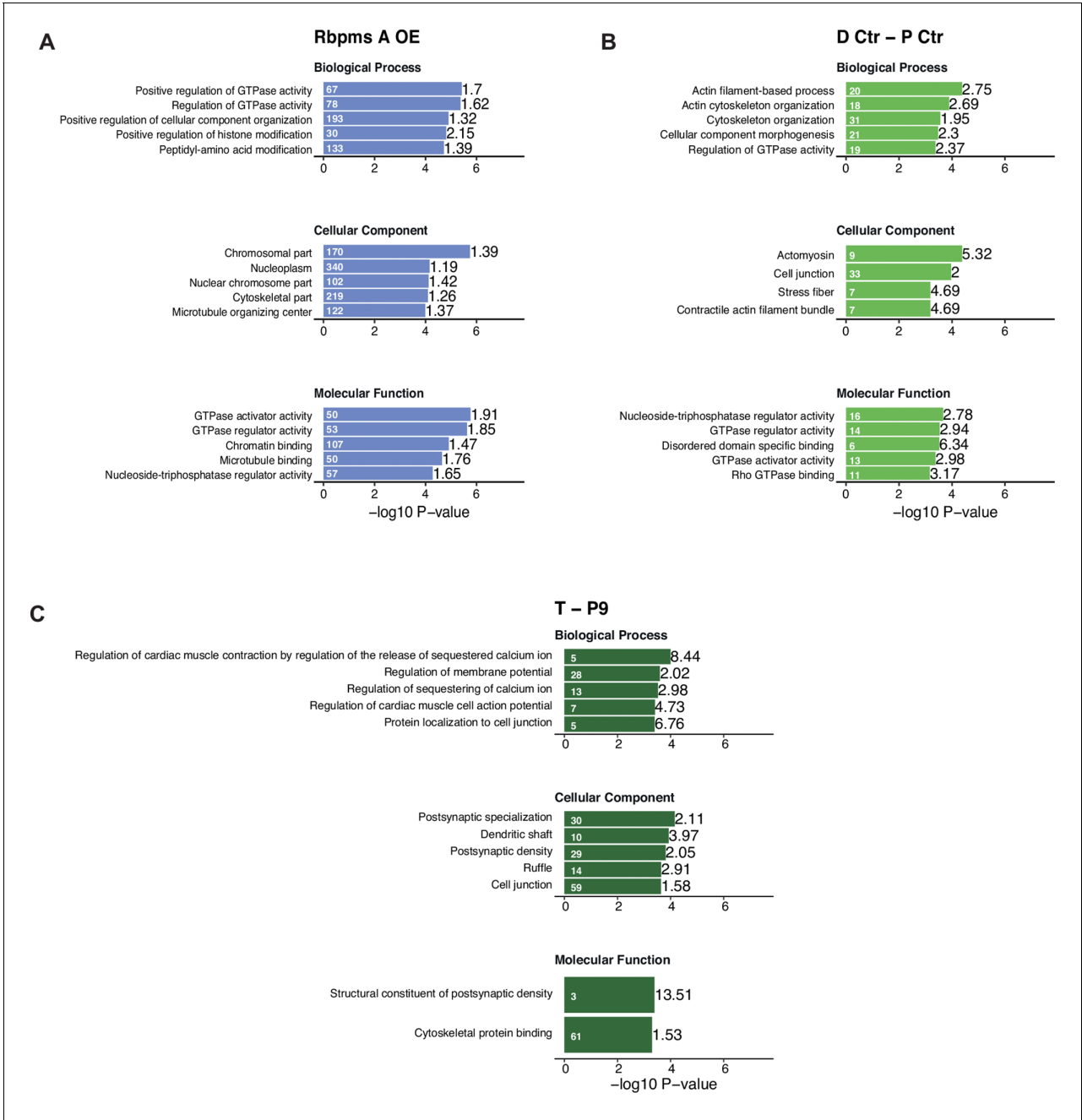


Figure 5—figure supplement 1. GO analysis of genes differentially spliced upon RBPMS overexpression and PAC1 and aorta dedifferentiation. Top five enriched GO terms from Gorilla GO analysis of differentially spliced genes. (A) RBPMS overexpression in proliferative PAC1 cells. (B) PAC1 dedifferentiation. (C) Rat aorta tissue dedifferentiation. Values within and in front of the bars indicate the number of genes in the enriched term and the enrichment relative to the background list.

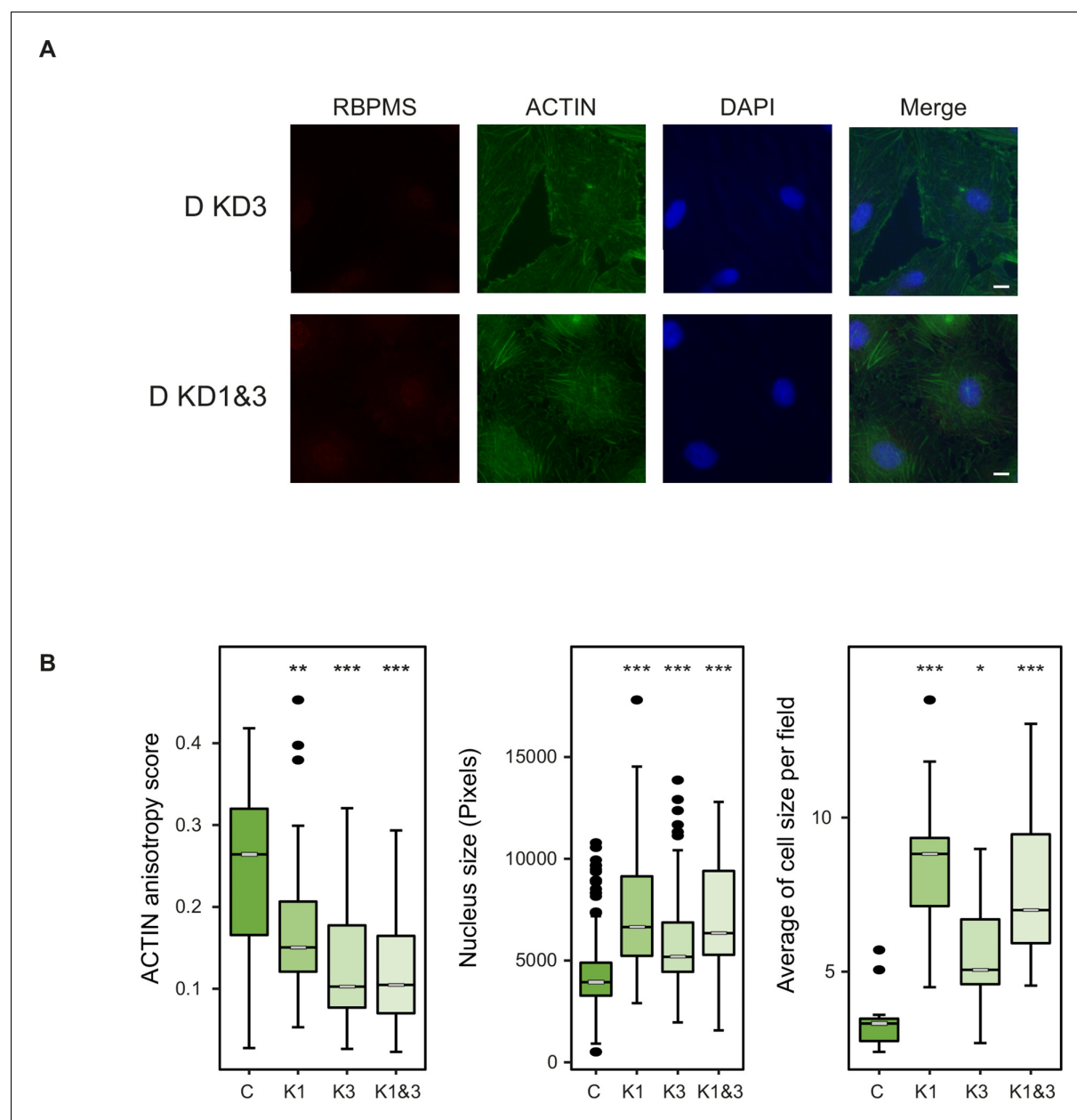


Figure 5—figure supplement 2. Morphological changes in PAC1 cells are specific to RBPMS knockdown. (A) Immunofluorescence of RBPMS and ACTIN (Phalloidin) in PAC1 cells treated with a second siRNA only (KD3, Stealth siRNAs, Thermo Fisher Scientific (RSS363830): CAG UAC UCC UCU GCC CAA CAC UGU A) and combined with siRNA1 (KD1 and 3–45 pmols of each) after 120 hr siRNA treatment. DAPI staining for cell nuclei. Scale bars 10 μ m. (B) Left, anisotropy measurement of ACTIN fibers in RBPMS knockdown (C, K1, K3 and K1 and 3) using the FibrilTool ImageJ macro (n = 56, 33, 26, 33, respectively). Middle, nucleus size measurement shown in pixels (n = 363, 75, 82, 93, respectively). Right, average of the cell size quantified per field (n = 14, 10, 7, 10). Statistical significance was obtained from a Mann-Whitney-Wilcoxon Test (*p<0.05, **p<0.01, ***p<0.001). Data shown are from one representative experiment carried out in triplicate.

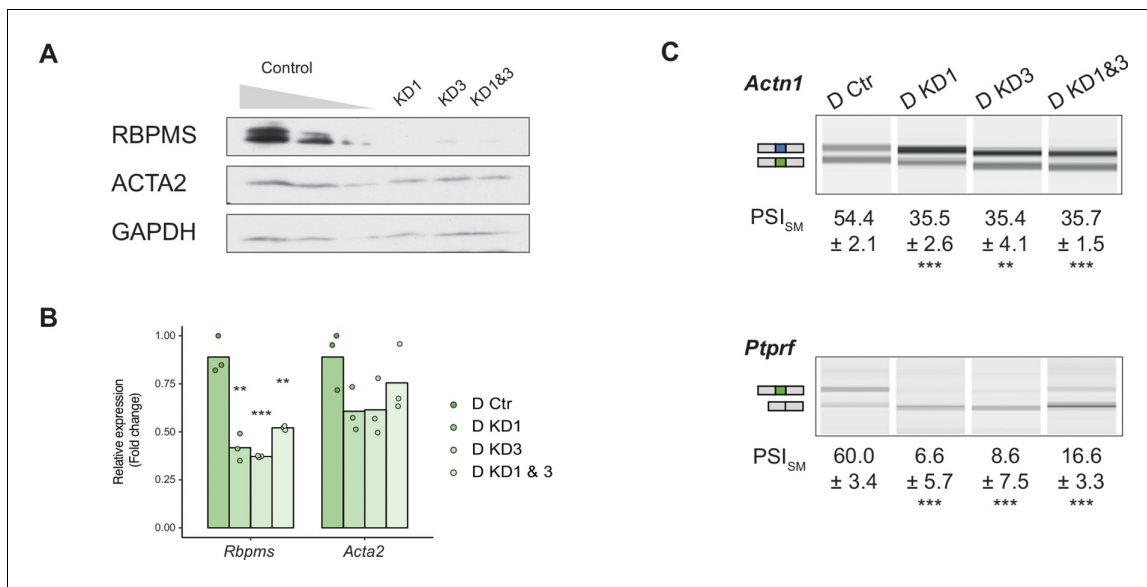


Figure 5—figure supplement 3. Sustained RBPMS knockdown in PAC1 cells. (A) Western blots showing RBPMS knockdown in PAC1 cells after 120 hr siRNA treatment (control (C), siRNA1 (KD1), siRNA3 (KD3), siRNA1 and 3 (KD1 and 3)). Antibody targeting ACTA2, a SMC differentiation marker, and GAPDH was used as loading control. (B) qRT-PCR analysis of *Rbpms* (all isoforms), and the SMC differentiation marker *Acta2*, in knockdown (control (C), siRNA1 (KD1), siRNA3 (KD3), siRNA1 and 3 (KD1 and 3)). Relative expression was normalized to the average of two housekeepers (*Gapdh* and *Rpl32*) and the mean of the relative expression is shown ($n = 3$). Each point shows data from an individual sample. Changes in *Acta2* were not significant. (C) RT-PCR analysis of RBPMS splicing targets *Actn1* and *Ptprf*, in PAC1 cells after 120 hr RBPMS KD. Schematic of the regulated isoform products on the left. Values shown are the quantified PSI (percent spliced in) of the smooth muscle isoforms (SM). Data are from one representative experiment performed in triplicate. Statistical significance was assessed using Student's t-test (* $p < 0.05$, ** $p < 0.01$, *** $p < 0.001$).

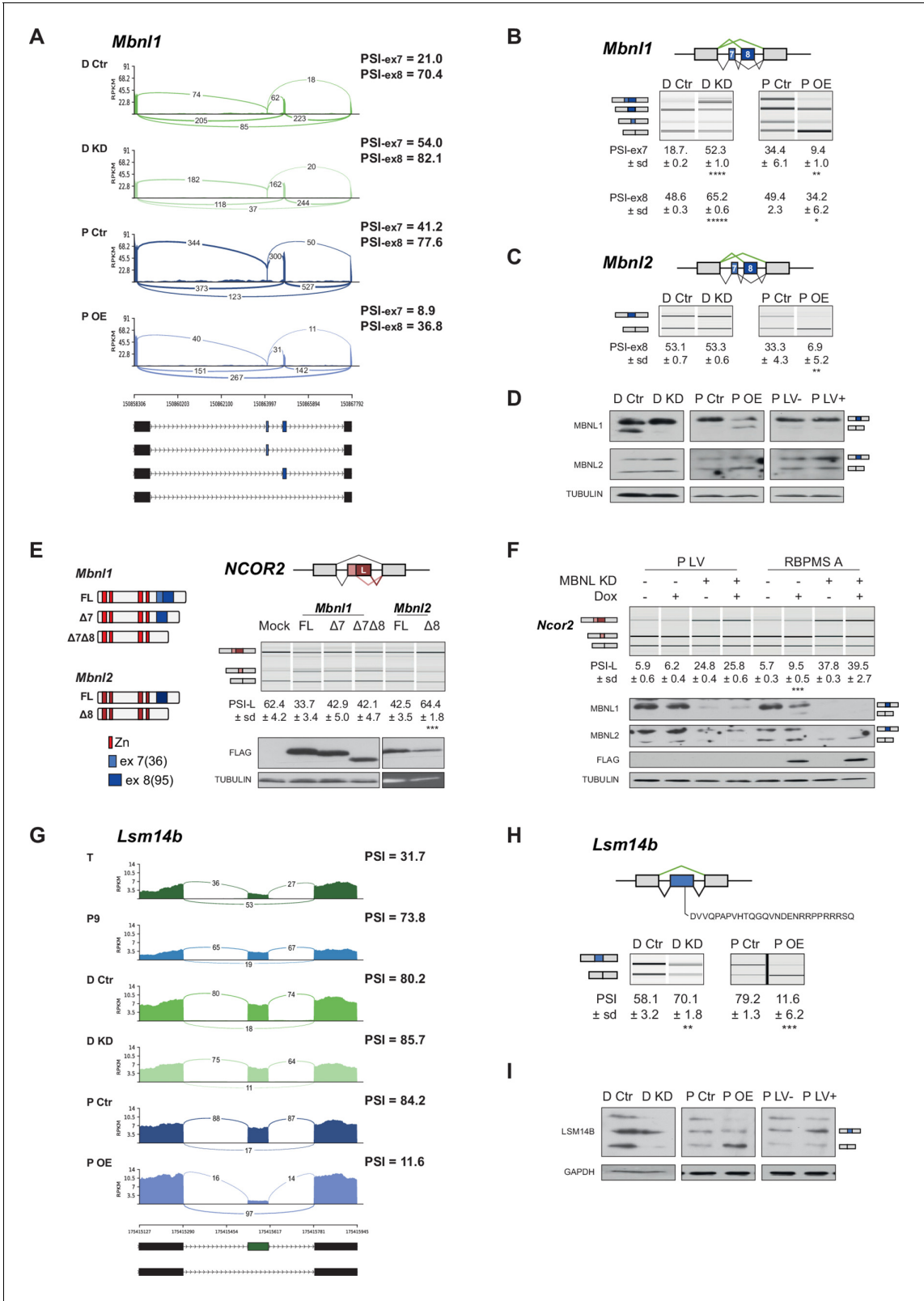


Figure 6. RBPMS regulates splicing of post-transcriptional regulators. **(A)** Sashimi plot of *Mbnl1* regulated exons. The numbers on top of the arches indicate the number of reads mapping to the exon-exon junctions. Mean of the PSI values calculated for each exon (exon 7–36 bp and exon 8–95 bp) are indicated for each condition (PSI-ex7 and PSI-ex8). Schematic of the different mRNA isoforms are found at the bottom. **(B)** RT-PCR validation of *Mbnl1* exons 7 and 8 and **(C)** *Mbnl2*. Values shown are the mean of the PSI ± standard deviation ($n = 3$). The PSI values for each exon of *Mbnl1* are *Figure 6 continued on next page*

Figure 6 continued

shown. For *Mbnl2*, exon seven isoforms were not detected in the RT-PCRs. Schematics of the splicing isoforms identify the PCR products. (D) Western blot probing for MBNL1 and 2 in RBPMS knockdown and overexpression shows the MBNL1 isoform switch at the protein level. (E) Schematic of the different MBNL1 protein isoforms, left. Different MBNL1 and MBNL2 isoforms were overexpressed in HEK293T cells and their effect on an A5SS event in the *NCOR2* gene assessed. Schematics of *NCOR2* splicing isoforms indicates the PCR products. Western blot were probed against FLAG to verify isoform overexpression. PSI indicates use of the downstream A5SS to generate the longer isoform. (F) MBNL1 and 2 knockdown in inducible RBPMS A or in lentiviral control (P LV) proliferative PAC1 cells to assess the dependency of the *Ncor2* A5SS event to the MBNL1 isoform switch. Western blot for MBNL1 and 2 and FLAG to confirm MBNL knockdown and RBPMS A overexpression. In all the western blots TUBULIN was used as a loading control. Statistical significance was calculated using Student's t-test (* $p < 0.05$, ** $p < 0.01$, *** $p < 0.001$). (G) Sashimi plot of the *Lsm14b* cassette exon regulated by RBPMS. PSI values represent the mean of the PSI values calculated by rMATS analysis. (H) RT-PCR validation of *Lsm14b* in the RBPMS knockdown and overexpression in PAC1 cells. Schematic of the *Lsm14b* event at the top and schematic of its isoforms at the left. Peptide sequence coded by the exon is shown below the schematic. (I) Western blot of LSM14B in RBPMS knockdown and overexpression cells. GAPDH was used for loading control.

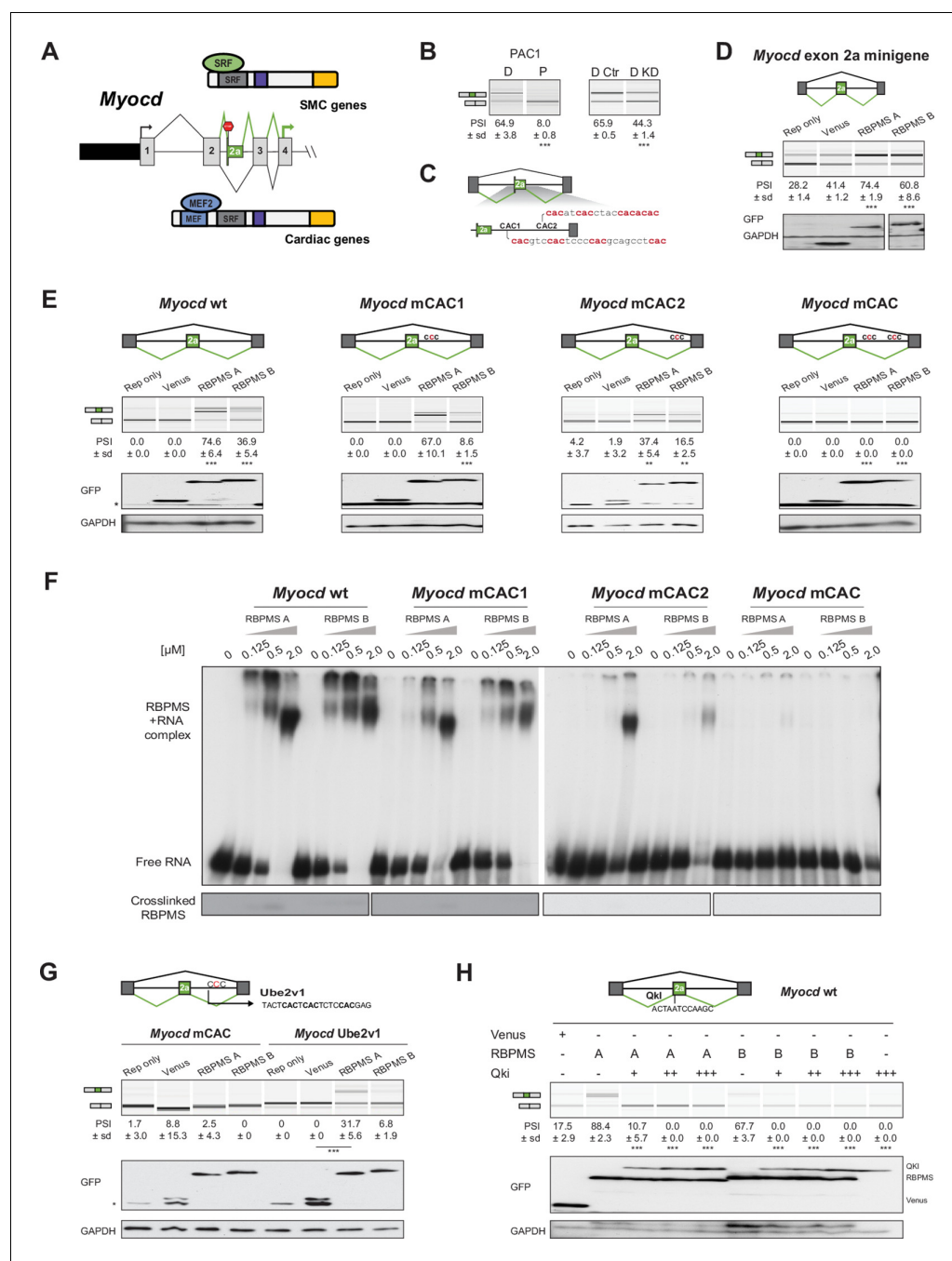


Figure 7. RBPMS controls splicing of the SMC transcription factor *Myocd* exon 2a. (A) Schematic of *Myocd* exon 2a ASE and its functional consequences upon MYOCD protein domains. (B) RT-PCR of *Myocd* exon 2a splicing in the PAC1 Differentiated (D) and Proliferative (P) PAC1 cells, left, and in differentiated PAC1 cells treated with control (D Ctr) or RBPMS siRNAs (D KD), right. (C) Schematic of the *Myocd* exon 2a splicing reporter. The two main clusters of CAC motifs, found downstream of exon 2a, are highlighted in red. (D) RT-PCRs of the effects of RBPMS A and B overexpression on *Myocd* exon 2a in PAC1 cells. Reporter only and Venus controls were tested alongside. Protein expression levels are shown in the western blot probing for GFP and GAPDH as a loading control. (E) RT-PCR of the effects of RBPMS A and B overexpression on *Myocd* exon 2a splicing reporter in HEK293. RBPMS CAC sites were mutated and response to RBPMS validated by RT-PCR. Schematic of the different mutant *Myocd* exon 2a splicing reporters are found at the top. RBPMS overexpression was confirmed by western blot using GAPDH as a loading control. (F) In vitro binding of RBPMS A and B to *Myocd* exon 2a downstream intron sequence in EMSA, top, and in UV-crosslink, bottom. In vitro transcribed wild-type and different mCAC

Figure 7 continued on next page

Figure 7 continued

RNAs were incubated with recombinant RBPMS (0.125 to 2 μ M). (G) The UBE2V1 sequence identified to bind to RBPMS by PAR-CLIP (**Farazi et al., 2014**) was inserted into the mCAC Myocd reporter. Schematic of the mCAC Myocd exon 2a splicing reporter and the UBE2V1 sequence. RT-PCR of the effects of RBPMS A and B overexpression on Myocd reporter in HEK293 cells. Western blot probing for GFP and GAPDH as a loading control. (H) Effects of the co-expression of RBPMS and QKI, a Myocd exon 2a repressor, on Myocd exon 2a reporter in HEK293. Myocd 2a reporter schematic with QKI and potential RBPMS-binding sites indicated. RBPMS and QKI overexpression was confirmed by western blot against GFP and GAPDH as a loading control. In GFP western blots, “*” indicates the GFP product from the splicing reporter.